Biaxial fatigue tests of notched specimens for AISI 304L stainless steel

G. Beretta, V. Chaves, A. Navarro
University of Sevilla. Departamento de Ingeniería Mecánica y Fabricación. Escuela Técnica Superior de Ingeniería. Universidad de Sevilla. Avda. Camino de los Descubrimientos, s/n. 41092, Sevilla. Spain.
guido.bere@gmail.com, chavesrv@us.es, navarro@us.es

ABSTRACT. High cycle fatigue tests were conducted for stainless steel AISI 304L. The geometry was a thin walled tube with a passing through hole. The tests were axial, torsional and in-phase axial-torsional, all of them under load control with R = −1. The S-N curves were constructed following the ASTM E739 standard and the fatigues limits were calculated following the method of maximum likelihood proposed by Bettinelli. The crack direction along the surface was analysed, with especial attention to the crack initiation zones. The notch fatigue limits for different hole diameters were compared with the predictions done with a microstructural fracture mechanics model.

KEYWORDS. Fatigue limit; Biaxial tests; Notch; Crack direction.

INTRODUCTION

Stress concentrations are the cause of fatigue failure in many industrial components. During the last few decades a great effort has been done by many researchers to understand the notch behaviour, either testing materials with notched geometries and/or proposing models to make predictions. Just focusing in the high cycle fatigue regime and the fatigue limit, many experimental works can be found in the literature: Gough tested V-notches in cylindrical specimens under combined stresses [1], Frost did tests on double V-notch flat plates made of mild steel [2], El Haddad et al. [3] and DuQuesnay et al. [4] did push-pull tests in plates with circular holes, Lukás et al. did push-pull tests of cylindrical specimens with circumferential semi-circular notches in 2.25Cr-1Mo steel and copper [5], Tanaka and Akinawa tested plates with elliptical notches [6], Meneghetti et al. tested double U-notch plates [7]. Susmel and Taylor conducted experiments using V-shaped notches loaded in tension at various angles of inclination [8] and Endo tested cylindrical specimens with a small surface hole, under axial, torsional and combined axial-torsional loading [9].
Many methods have been proposed to predict the fatigue limit of notches under multiaxial fatigue loading, as the square root of the defect area method proposed by Murakami and Endo to deal with defect-containing components [10], the Point Method of Taylor using the Susmel-Lazzarin critical plane criterion [8], the damage model extended to stress gradients proposed by Brighenti and Carpinteri [11], or the extension of the short crack growth model of Navarro and de los Rios [12] to specimens containing holes under in-phase biaxial loading [13].
However, despite all this work, it is a fact that the mechanisms of fatigue crack growth at notches are still not fully understood. In particular, it still remains unclear the direction of the crack during the initial growth of the crack, known as

Stage I. According to the critical plane approaches, the Stage I occurs on the maximum shear stress plane. Susmel and Taylor [8] conducted experiments using V-notches at various angles of inclination to reproduce a multiaxial loading condition, and observed that the Stage I crack growth occurred on the plane of maximum shear stress. Endo [9], conducted tests on cylindrical specimens with a small surface hole, under axial, torsional and combined axial-torsional loading and observed that the crack grew approximately normal to the first principal stress from the start, regardless of the applied stress. So, these two experimental studies show a disagreement in the Stage I direction. The knowledge of this direction is crucial, as most of the methods for predicting the fatigue limits are based on a stress gradient along a certain line, which is supposed to be representative of the Stage I crack path.
This paper reports on an experimental study conducted with stainless steel AISI 304L under proportional biaxial loading, from pure tension to pure torsion, in the high-cycle-fatigue regime. The geometry was a thin walled tube with a passing through hole. The direction of the crack on the specimen surface was examined. Finally, theoretical predictions were compared with the experimental results.

MATERIAL DATA AND TESTS

The material was commercial AISI 304L stainless steel. Its chemical composition (in wt.%) was as follows: 0.021 C, 0.029 P, 0.024 S, 0.34 Si, 1.485 Mn, 18.227 Cr, 8.148 Ni, 0.215 Mo, 0.0005 Ti, 0.08 N and 0.39 Cu. The microstructure was formed by equiaxed austenite grains with some delta ferrite bands and the average austenite grain size was 80 μm. The specimens were machined from 22-mm-diameter round bars. No heat treatment was applied after the machining. The monotonic mechanical properties, as determined from 5 tensile tests, were as follows: tensile strength, σ_{UTS} = 654 MPa; yield strength, σ_{YS} (0.2%) = 467 MPa; and elongation, A = 56%. Fatigue tests were performed either in a servo-hydraulic axial–torsion load frame, at a frequency of 6-8 Hz, or in a resonance testing machine, at 80-100 Hz, in both cases under fully-reversed loading (R =-1). Each test was completed when the crack grew to be several millimetres long or after 3.5×10^6 cycles (run-outs). The fatigue limit in tension–compression (R = -1), as determined for cylindrical specimens and expressed in terms of stress amplitude, was σ_{FL} = 316 MPa, and the torsional fatigue limit τ_{FL} = 288 MPa (for further details, please see [14]). The fatigue limits were calculated using the method proposed by Bettinelli [15], an alternative to classical choices such as the staircase method. The probability of being a run-out is expressed by a binomial distribution, and the value of the fatigue limit is estimated using the maximum likelihood method.

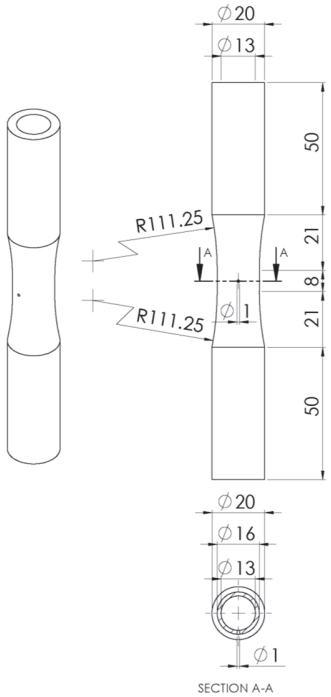

Figure 1: Geometry of the notched specimen with the passing through hole.

The geometry of the notched specimen was a thin walled tube with a passing through hole (see Fig. 1). The diameters d of the holes were 1, 2 and 3 mm. The external surface of the gauge section was carefully polished to remove machining marks until reaching an average roughness (Ra) of 0.1 μm. The passing hole and the internal surface of the tube were machined with great care. Unfortunately, it was not possible to polish these two surfaces.

FATIGUE LIMIT PREDICTIONS WITH THE MICROSTRUCTURAL MODEL

Navarro and de los Rios [12] developed a model for short fatigue cracks growing in un-notched bodies. The authors assumed that plastic displacement ahead of the crack take place in rectilinear slip bands cutting across the grains of the material. This model was recently applied to a circular notch under proportional biaxial loading [13]. The problem is sketched in Fig. 2. For simplicity, the remote applied stresses σ_y^∞, τ^∞ defining the biaxial load are considered to range between 0 and 1. The crack and the barrier, which represents the grain boundary, are modeled with dislocations. To keep the symmetry in the problem two opposing cracks are considered. The crack is modeled as a straight line and its initiation point and its direction can be whatever, defined by the angles θ and θ_1. The solution of the equilibrium equations for the two distributions of dislocations (one with Burger's vector perpendicular to the crack and the other parallel to the crack) under the remote applied stresses, provides the stresses at the barrier, σ_3^i and τ_3^i, for successive crack lengths (a=iD/2), which are expressed in terms of half grains D (i=1,3,5,...). These barrier stresses depend linearly on the applied stresses, as it was shown in a previous publication [16]. Then, the value of the load required to overcome the i-th barrier, $\lambda(\theta, \theta_1, i)$ is just the value that multiplied by the stresses at the barrier lead to the fulfilment of the biaxial activation criterion, which has the following expression:

$$\lambda(\theta,\theta_1,i)=\frac{1}{\dfrac{\sigma_3^i}{m_{\sigma i}^{*}\cdot\tau_c}+\dfrac{\tau_3^i}{m_{\tau i}^{*}\cdot\tau_c}} \tag{1}$$

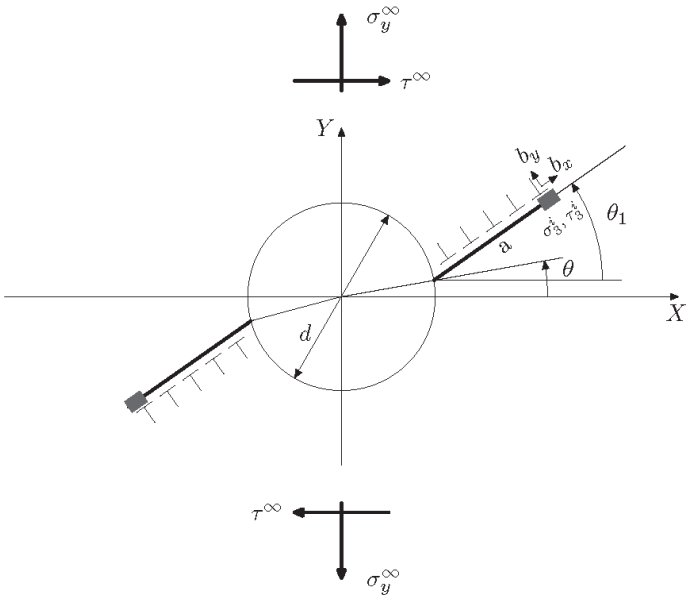

Figure 2: Sketch of the microstructural model applied to an infinite plate with a circular hole subjected to proportional biaxial loading.

In the previous expression, $m_{\sigma i}^{*}\cdot\tau_c$ and $m_{\tau i}^{*}\cdot\tau_c$ are the activation constants, which depends on the material and can be calculated from the plain fatigue limits in tension and torsion and the Kitagawa diagram. The maximum value of λ for all these crack lengths a=iD/2 (i=1, 3, 5, ...) will provided the minimum load $\lambda(\theta, \theta_1)$, required to overcome all the barriers along the direction defined by the angles θ and θ_1. As an estimation this maximum value is generally reached for a crack

length that oscillates between 1 and 10 grain diameters, depending on the material, the stress gradient ahead of the notch, etc. This procedure must be repeated for all the directions given by θ and θ_1 and the minimum value of all the obtained $\lambda(\theta, \theta_1)$, will be the predicted notched fatigue limit, λ_0^N:

$$\lambda_0^N = \min\left\{\lambda\left(\theta,\theta_1\right)\right\} \tag{2}$$

The values of θ, θ_1 for λ_0^N will provide the predicted crack initiation point at the notch and the predicted crack direction along the first grains (Stage I). For a full explanation of the microstructural model applied to a circular notch under proportional biaxial loading, please see the reference [13].

EXPERIMENTAL RESULTS AND PREDICTIONS

The experimental fatigue limits for the AISI 304L stainless steel and the predictions with the microstructural model are shown in Fig. 3. There are results for three hole diameters, d=1 mm, d=2 mm and d=3 mm. Besides, the experimental data for smooth specimens, already published [14], and its theoretical curve (ellipse quadrant) is plot. It is seen that the predictions for d=2 mm agree quite well with the experimental data, while for d=1 mm and d=3 mm the agreement is not so good. More experimental data is required to get a reliable evaluation of the model.

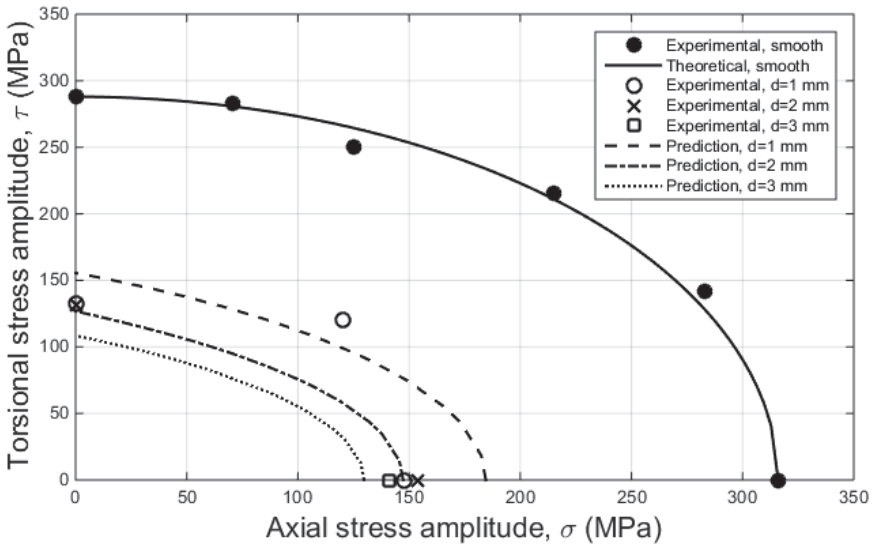

Figure 3: Comparison of experimental and predicted fatigue limits for the AISI 304L stainless steel.

Crack initiation point and crack direction during the Stage I

Figs. 4, 5 and 6 show examples of cracks emanating from the hole for tension-compression, pure torsion and in-phase biaxial loading ($\sigma_y^\infty = \tau^\infty$), respectively, for applied stresses close to the fatigue limit. The crack initiation point was, in the majority of the tests, located close to the point of maximum principal stress, which according to Fig. 2, means a value of θ=0º for the axial tests, θ=45º for the torsion tests and θ=31.7º for the biaxial tests ($\sigma_y^\infty = \tau^\infty$). The crack direction along the first 400 μm (5 average grains long), considered as the Stage I of the crack growth, was also studied. The experimental directions were close to the maximum principal stress direction, which means values of θ_1=0º for axial tests, θ_1=45º for torsional tests and θ_1=31.7º for biaxial tests ($\sigma_y^\infty = \tau^\infty$). With respect to the model, an approximately similar minimum value of λ is obtained for several combinations of θ, θ_1. It means that the predicted notched fatigue limit, λ_0^N, is associated with several initiation points and crack directions. Certainly, this is not fully correct, as the experimental values of θ, θ_1 are quite precise and with low scatter. Further work needs to be done in the model in order to discriminate directions and correctly predict the crack initiation point and the Stage I crack direction.

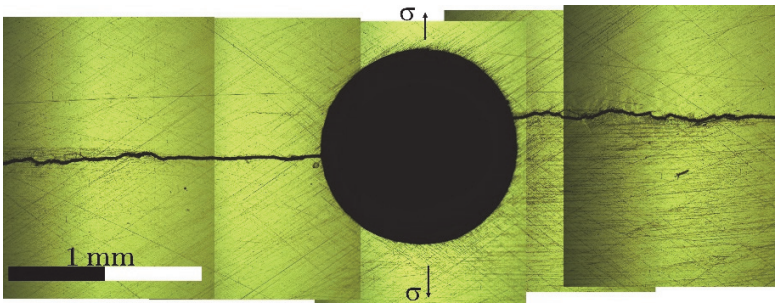

Figure 4: Tension-compression. Cracks emanating from the hole at an applied stress close to the fatigue limit. d = 1 mm, σ_y^∞ = 200 MPa, N = 308 700 cycles.

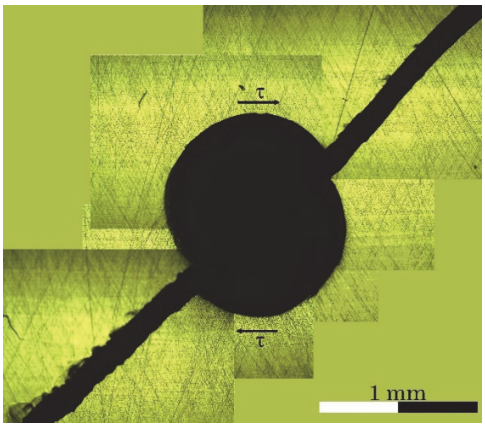

Figure 5: Cracks emanating from the hole at an applied stress close to the fatigue limit. d = 1 mm, τ^∞ = 146 MPa, N = 1 454 269 cycles.

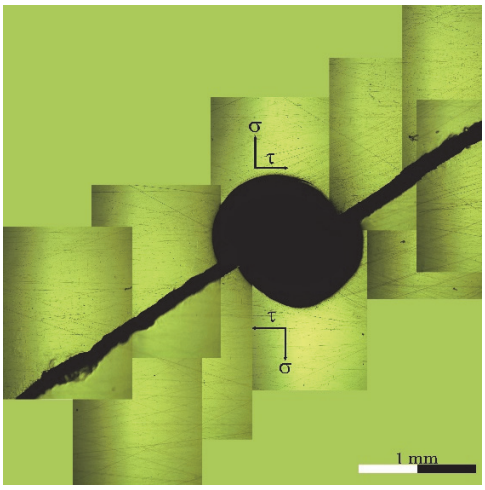

Figure 6: Cracks emanating from the hole at an applied stress close to the fatigue limit. d = 1 mm, $\sigma_y^\infty = \tau^\infty$ = 140 MPa, N = 206 765 cycles.

Conclusions

An experimental program has been conducted for tubes with a passing through hole of AISI 304L stainless steel under in-phase biaxial loading. Biaxial fatigue curves were constructed using the experimental fatigue limits. The predictions of the fatigue limits obtained with a microstructural model reasonably agreed with the experimental

values. The crack initiation point was close to the point of maximum stress, that is, 0º for axial tests and 45º for torsional tests. The crack direction along the Stage I was close to the maximum principal stress direction.

ACKNOWLEDGEMENTS

The authors would like to thank the Spanish Ministry of Education for its financial support through grant DPI2014-56904-P.

REFERENCES

[1] Gough, H.J, Pollard, H.V., Clenshaw, W.J., Ministry of Supply, Aeronautical Research Council Reports and Memoranda. London: His Majesty's Stationary Office (1951).
[2] Frost, N.E., Proc Instn Mech Eng, 173 (1959) 811-827.
[3] El Haddad, M.H., Topper, T.H., Smith, K.N., Prediction of Non-Propagating Cracks Eng Fract Mech, 11 (1979) 573-584.
[4] Duquesnay, D.L., Yu, M.T., Topper, T.H., in: The behaviour of short fatigue cracks, Miller, K.J, de los Rios, E.R. (Ed), Elsevier, (1986) 323-335.
[5] Lukás, P., Kunz, L., Weiss, B., Stickler, R., Fatigue Fract Engng Mater Struct, 9 (1986) 195-204.
[6] Tanaka, K., Akinawa, Y., in: Fatigue'87. Ritchie, R.O., Starke Jr., E.A. (Ed), Engineering Materials Advisory Services, (1987) 739-748.
[7] Meneghetti, G., Susmel, L., Tovo, R., High-cycle fatigue crack paths in specimens having different stress concentration features, Eng Failure Anal, 14 (2007) 656-672.
[8] Susmel, L., Taylor, D., wo methods for predicting the multiaxial fatigue limits of sharp notches, Fatigue Fract Engng Mater Struct, 26 (2003) 821-833.
[9] Endo, M. (2003), in: Biaxial/Multiaxial Fatigue and Fracture, ESIS publication 31, Carpinteri, A., de Freitas, M. and Spagnoli, A. (Ed), Elsevier, (2003) 243-364.
[10] Murakami, Y., Endo, M., Effects of defects, inclusions and inhomogeneities on fatigue strength, Int J Fatigue, 16 (1994) 163-82.
[11] Brighenti, R, Carpinteri, A., A notch multiaxial-fatigue approach based on damage mechanics, Fatigue Fract Engng Mater Struct, 39 (2012) 122-133.
[12] Navarro, A., de los Rios, E.R., Philos Mag A, 57 (1988) 12-36.
[13] Chaves, V., Navarro, A., Beretta, G., Madrigal, C., Microstructural model for predicting high cycle fatigue strength in the presence of holes under proportional biaxial loading, Theor Appl Fract Mech, 73 (2014) 27-38.
[14] Chaves, V., Navarro, A., Madrigal, C., Stage I crack directions under in-phase axial–torsion fatigue loading for AISI 304L stainless steel, Int J Fatigue, 80 (2015) 10-21.
[15] Bettinelli, S., Tesi di Laurea, Universita degli studi di Padova. Supervisor: Prof. R. Tovo, (2006).
[16] Chaves, V., Navarro, A., Fatigue limits for notches of arbitrary profile, Int J Fatigue, 48 (2013) 68-79.